Published in final edited form as:
Inorg Chem. 2011 February 21; 50(4): 1506–1512. doi:10.1021/ic1020719.

Coordination-Driven Self-Assembly of M_3L_2 Trigonal Cages from Pre-organized Metalloligands Incorporating Octahedral Metal Centers and Fluorescent Detection of Nitroaromatics

Ming Wang[†], **Vaishali Vajpayee**[‡], **Sankarasekaran Shanmugaraju**[§], **Yao-Rong Zheng**[†], **Zhigang Zhao**[†], **Hyunuk Kim**[⊥], **Partha Sarathi Mukherjee**[§], **Ki-Whan Chi**[‡], and **Peter J. Stang**[†]

Peter J. Stang: stang@chem.utah.edu

[†]Department of Chemistry, University of Utah, 315 South 1400 East Salt Lake City, Utah 84112

[‡]Department of Chemistry, University of Ulsan, Ulsan 680-749 Republic of Korea

[§]Inorganic and Physical Chemistry Department, Indian Institute of Science, Bangalore-560012, India

[⊥]Department of Chemistry, POSTECH, Pohang, 690-784, Republic of Korea

Abstract

The design and preparation of novel M_3L_2 trigonal cages via coordination-driven self-assembly of pre-organized metalloligands containing octahedral aluminum(III), gallium(III), or ruthenium(II) centers is described. By employing tritopic or dinuclear linear metalloligands and appropriate complementary subunits, M_3L_2 trigonal-bipyramidal and trigonal prismatic cages are self-assembled under mild conditions. These 3-D cages were characterized with multinuclear NMR spectroscopy (^{1}H and ^{31}P) and high-resolution electronic spray mass spectrometry (HR-ESI-MS). The structure of one such trigonal prismatic cage, self-assembled from an arene ruthenium metalloligand, was confirmed via single-crystal X-ray crystallography. The fluorescent nature of these prisms, due to the presence of their electron-rich ethynyl functionalities, prompted photophysical studies which revealed that electron-deficient nitroaromatics are effective quenchers of the cages' emission. Excited state charge transfer from the prisms to the nitroaromatic substrates can be used as the basis for developing selective and discriminatory turn-off fluorescent sensors for nitroaromatics.

Keywords

Coordination-driven self-assembly; Metalloligands; Three-dimensional cages; Nitroaromatics detection

Introduction

Three-dimensional supramolecular entities are ubiquitous throughout nature and account for various biological functions. For example, viral capsids are precisely assembled cages

Correspondence to: Partha Sarathi Mukherjee; Ki-Whan Chi; Peter J. Stang, stang@chem.utah.edu.

Supporting Information Available: ^{1}H and ^{31}P{^{1}H} NMR spectra of trigonal-bipyramidal cages **6** – **8**; ESI mass spectra for cages **7** and **8**; ^{1}H NMR spectra of **12** and **13**; crystal file information of **12** (in CIF format); spectral and photophysical data of **12** and **13** in methanol; crystallographic file (in CIF format) of **12**. This material is available free of charge via the Internet at http://pubs.acs.org.

comprised of protein subunits and serve the biological role of nucleic acid storage.[1] In the past two decades, weak noncovalent and dative metal-ligand interactions have been exploited using appropriately designed molecular subunits in a predictive manner to construct aesthetically appealing abiological 3-D self-assemblies.[2] This approach has also provided access to functional materials with a wide range of desirable structural and dynamic properties.[3] The construction of functional supramolecular architectures possessing tailor-made properties, such as molecular recognition,[4] host-guest chemistry,[5] and supramolecular catalysis[3f,6] has become the focus of modern metallosupramolecular chemistry. Transition metal-mediated, coordination-driven self-assembly has emerged as a useful synthetic tool to access such species. For example, hydrophobic or fluorous nanophases were accessed by endofunctionalized $M_{12}L_{24}$ molecular spheres assembled by this route.[7a] Additionally, similarly formed chiral metal-organic tetrahedral cages have separated racemic mixtures with high enantioselectivity.[7g]

To date, the directional bonding approach for the coordination-driven self-assembly of 3-D metallosupramolecules has proven quite successful and focuses on the use of rigid, organic ligands encoded with information on directionality and angularity. More recently, interest in the application of pre-organized metallocomplexes to direct coordination-driven self-assembly and the preparation of metallosupramolecules has increased.[8–11] Self-assemblies constructed from such building blocks can introduce unique characteristics such as magnetic[8d] or photophysical properties and chiral centers,[8e] while avoiding the time-consuming and expensive multi-step syntheses required to install these attributes via conventional synthetic pathways. We have previously shown that 2-D polygons can be constructed from the coordination-driven self-assembly of metalloligands.[12] For example, a [5 + 5] pentagon was prepared from 108° metal-carbonyl dipyridine ligands[12], [3 + 3] hexagons and [2 + 2] rhomboids containing cobalt carbonyl motifs have been prepared via supramolecule-to-supramolecule transformations of ethynyl functionalized building blocks.[12b] We now report on the extension of this approach to 3-D assemblies.

Square planar Pd(II) and Pt(II) metals have been exploited for their structural rigidity in the synthesis of several discrete structures of predefined shapes and sizes.[2,3] Octahedral metal ions are known to be less predictable for construction of defined discrete structures. But constructing discrete metallosupramolecules via the self-assembly of transition-metal complexes with octahedral geometries is a growing field due to the versatile properties expected in the presence of such metal ions.[8, 11–12] Application of octahedral and square planar metal ions together to the generation of discrete and defined structures has not been well explored. In continuation of our investigation into the scope and diversity of functional metallosupramolecules, herein we present M_3L_2 3-D trigonal bipyramidal cages that are assembled from pre-organized metalloligands containing octahedral aluminum(III) and gallium(III) centers (Scheme 1) in combination with Pt(II) acceptors. M_3L_2 cages represent the simplest 3-D supramolecular structures[13] and can be assembled by the combination of two tritopic subunits and three ditopic tectons.[14] To further explore the self-assembly of M_3L_2 cages in a complementary way using octahedral metalloligands, we report the reactions of octahedral Ru(II) metal containing bidentate acceptors with tridentate pyridyl donor 1,3,5-tris(4-pyridylethynyl)benzene to afford M_3L_2 trigonal prisms.

In this paper, octahedral complexes **1** and **2**, prepared from 4-pyridylbutane-1,3-dione and cationic gallium(III) and aluminum(III), respectively, were employed as tritopic ligands for the assembly of trigonal-bipyramidal cages (Scheme 1, A). Treatment of cationic gallium(III) or aluminum(III) with 4-pyridylbutane-1,3-dione results in coordination of the latter's β-diketone moiety, poising the three pyridine groups of **1** or **2** to subsequently bind additional metal centers. Furthermore, the pyridine rings are oriented orthogonal to one another due to the octahedral coordination environment about the metal centers, permitting

three dimensional growth.[8a, 8e] Thus, when octahedral metal containing donors **1** and **2** are combined with 90° or 60° platinum acceptors, M_3L_2 type heterometallic trigonal bipyramidal cages are formed. In a complementary approach, dinuclear half-sandwich octahedral Ru(II) arene acceptors **10** and **11**[15−16] were combined with 1,3,5-tris(4-pyridylethynyl)benzene **9** to assemble M_3L_2 trigonal prismatic cages (Scheme 1, B). The ethynyl groups built into ligand **9** impart electron-rich and fluorescent properties to cages **12** and **13**. Using UV-Vis and fluorescence emission spectral analysis, we investigated the host-guest properties of cages **12** and **13** with electron deficient nitroaromatics. Upon addition of nitroaromatics, the emission of **12** and **13** was quenched, demonstrating the utility of these cages for development into selective and discriminatory fluorescence sensors for nitroaromatics.

Results and Discussion

Construction of M_3L_2 Heterometallic Trigonal-bipyramidal (TBP) Cages

The preparation of heterometallic trigonal-bipyramidal cages **5** and **6** was achieved by the [2 + 3] self-assembly of metalloligands **1** and **2**, respectively, with the 90° platinum acceptor **3**. Upon addition of a CD_2Cl_2 solution of ligand **1** or **2** into 1.5 equivalents of **3** in CD_3NO_2, **5** and **6** were afforded after 5 h of stirring at room temperature. Similarly, for the self-assembly of **7** and **8**, metalloligands **1** and **2** were treated with the 60° acceptor **4** in an acetone-d_6 and D_2O (v:v = 1:1) solution for 15 h at 65°C. $^{31}P\{^1H\}$ and ^1H NMR multinuclear analysis of the reaction mixtures revealed the formation of single, discrete species with high symmetry. The $^{31}P\{^1H\}$ NMR spectra of self-assemblies **5** – **8** display single, sharp singlets with concomitant ^{195}Pt satellites (−1.4 ppm for **5**, −0.3 ppm for **6**, 14.2 ppm for **7** and 11.8 ppm for **8**) shifted upfield (Δδ (ppm) = 14.0 for **5**, 12.9 for **6**, 4.1 for **7** and 6.5 for **8**) relative to starting platinum acceptors **3** or **4** (Figure 1A and Figure S1 in the Supporting Information (SI)). Compared to their signals before self-assembly, the resonances of the α- and β-protons of the pyridine rings show significant downfield shifts in the proton NMR spectra of these trigonal-bipyramidal cages (Figure 1B and Figure S2–S4, SI), due to the loss of electron density upon coordination to platinum. It is also notable that the doublets at 8.65 and 7.75 ppm, which were ascribed to the α- and β-protons of the pyridine ring in the coordinated cages of **5** and **6**, split into pairs of doublets. A similar split was observed for the doublet at 8.70 ppm corresponding to the α-protons of the pyridine rings of **7** and **8** (Figure S2 – S4 in SI). These results can be explained by the hindered rotation of the pyridine rings upon coordination to platinum, consistent with our previous reports.[15] The sharp NMR signals in both the ^{31}P and ^1H NMR spectra, along with the solubility of these species, ruled out the formation of oligomers in solution.

Further proof for the trigonal-bipyramidal structures of **5** – **8** was obtained using electrospray ionization mass spectrometry (ESI-MS). The ESI-MS spectrum of **5** exhibited two charged states at m/z = 1500.2 and 950.8, corresponding to $[M - 2OTf]^{2+}$ and $[M - 3OTf]^{3+}$, respectively. For assembly **6**, two charged states at m/z = 1457.3 and 654.7 were assigned to $[M - 2OTf]^{2+}$ and $[M - 4OTf]^{4+}$, respectively. Charged states at m/z = 1473.4 (**7**) and 1089.6 (**7**) and m/z = 1445.5 (**8**) and 1068.6 (**8**) were observed to correspond with $[M - 3NO_3]^{3+}$ and $[M - 4NO_3]^{4+}$ for these final two cages, **7** and **8**. These peaks were isotopically resolved and in good agreement with the calculated theoretical distributions (Figure 2 and Figure S5 in SI).

Although X-ray structural information was elusive for the trigonal-bipyramidal cages, the sizes and shapes **5** and **7** were ascertained from the results of MM2 force-field simulations (Figure 3). The calculated inner-cavity diameter of these cages was *ca.* 1.3 nm for **5** and *ca.* 1.8 nm for **7**.

Trigonal Prismatic Cages Self-assembled from Half-Sandwich Ruthenium(II) Metalloligands

Trigonal prismatic cages **12** and **13** were obtained by [2 + 3] self-assembly of the tritopic planar donor **9** with half-sandwich arene ruthenium(II) metalloligands **10** and **11**, respectively. A nitromethane solution containing **9** was added to a methanol solution of **10** or **11** in a 2:3 ratio and allowed to stir at room temperature for 4 h. Upon addition of diethyl ether into the concentrated reaction mixtures, **12** and **13** were precipitated as yellow and red-wine crystalline solids, respectively. The trigonal prismatic structures of **12** and **13** were confirmed by NMR and high-resolution mass spectra analysis. The molecular structure of **12** was further elucidated by single-crystal X-ray diffraction using synchrotron radiation. The ^{1}H NMR spectra of **12** and **13** exhibit two doublets (δ = 8.21 and 7.61 ppm for **12**, δ = 8.45 and 7.65 ppm for **13**), assigned to the pyridine protons of the self-assemblies. Additionally, sharp singlets at δ = 7.78 (**12**) and 7.84 ppm (**13**) were observed for the 2,4,6-protons of the central aromatic ring of **9**, and two doublets for the *p*-cymene moiety were observed at δ = 6.11 and 5.96 ppm for **12** and δ = 6.21 and 6.01 ppm for **13** (Figure S6, SI). The assignment of trigonal prismatic structures to **12** and **13** was also supported by electrospray ionization mass spectrometric analysis (Figure 4). Charged states at m/z = 1517.0 (**12**), 961.7 (**12**), 1592.8 (**13**), 1011.9 (**13**) were observed, corresponding to $[M - 2OTf]^{2+}$ and $[M - 3OTf]^{3+}$. These peaks were isotopically resolved and in good agreement with the calcualted theoretical distributions. After exchanging anions from a triflate to a perchlorate, a single-crystal of **12** suitable for X-ray analysis was obtained by slow vapor diffusion of diethyl ether into a dichloromethane/methanol solution of **12** (Table S1, SI). As shown in Figure 5, the two tritopic ligands are arranged face-to-face, coordinated to three arene ruthenium metalloligands to give a trigonal prismatic structure with a height of approximately 7 Å and distance of about 24 Å between the edges. Inspection of the crystal packing reveals that **12** has a 1-D columnar structure along the α-axis. Discrete trigonal prisms stack to give favorable π-π interactions with a 60° rotation between cages and an intermolecular spacing of 3.4 Å. The interstitial sites of the crystal structures for **12** are occupied by perchlorate counter anions and solvent molecules.

Photophysical studies of trigonal prismatic cages 12 and 13: fluorescent detection of nitroaromatics

Cages **12** and **13** (0.01 M in MeOH) exhibit strong bands at λ= 310 nm for **12** and λ= 315 nm for **13**, which are attributed to intra/inter molecular π-π* transitions. The absorption features of **12** exhibit dynamic behavior in the presence of nitroaromatics. The inclusion of electron rich ethynyl moieties rendered cage **12** fluorescent, therefore, electronic variations were monitored upon the addition of electron deficient nitroaromatics. When trinitrotoluene (TNT) was added to a solution of **12** (1.0×10^{-5} M in methanol), significant absorption changes in the UV-Vis spectra were observed, as shown in Figure 6. Upon addition of TNT, the strong absorption at 315 nm decreases in intensity while a new absorption at 250 nm gradually increases, reaching maximum at a TNT concentration of 72 μM. The well-anchored isosbestic point at 306 nm in the absorption spectra of **12** upon TNT addition indicates the formation of a stable complex between the **12** and TNT.

Solutions of **12** and **13** (1.0×10^{-6} M in methanol) are emissive when excited at 280 nm, the spectra of which exhibit three bands with wavelengths of 349 nm, 361 nm and 380 nm (Figure 7). The quantum yields of **12** and **13** were determined to be 0.12 and 0.22, respectively, relative to that of anthracene (Table 2, SI). The emission spectra were sensitive to the addition of nitroaromatics, which quenched the emission of the self-assemblies significantly. The fluorescence intensity of **12** decreased 70% in the presence of 148.9 μM TNT (Figure 7, *left*). The ratio of fluorescence intensity I_0/I (monitored at 350 nm), where I and I_0 represent the fluorescence intensity of **12** with and without TNT, respectively, show a

linear response to TNT concentration in the range of 0 to 150 μM (Figure 7, *right*). The Stern-Volmer constant K_{sv} was determined to be 2.1×10^4 M^{-1} by fitting the linear plot to the Stern-Volmer equation $I_0/I = 1 + K_{sv}[TNT]$. The stiochiometry and the binding constant of TNT/Cage 12 were determined to be 5:1 and 4.91×10^4 M^{-1}, respectively (Figure S7, S8, SI). Notably, the addition of 45.8 μM picric acid (PA) quenched the fluorescence of **12** completely compared to TNT under same conditions (Figure 8). In this case, the Stern-Volmer constant was determined to be 1.0×10^5 M^{-1}. This phenomenon can be explained by the electron deficient nature of PA relative to TNT, leading to a stronger electron transfer and ultimately more efficient quenching.[17–18]

When a variety of aromatic compounds such as benzoic acid (BA), 4-methoxybenzoic acid (4-MeOBA), 1, 4-benzoquinone (BQ), 4-nitrotoluene (NT), nitrobenzene (NB), 4-nitrophenol (NP), TNT and PA were added to solutions of **12** or **13**, only the nitroaromatics efficiently quenched the fluorescence emission, as shown in Figure 9. This result is consistent with the expected mode of π-π interactions, in which electron deficient nitroaromatics act as fluorescence quenchers either via excited state electron transfer from the electron rich prismatic cage **12** or **13** or by charge-transfer complex formation.

Conclusion

We present in this paper the construction of M_3L_2 trigonal cages via the coordination-driven self-assembly of pre-organized metalloligands containing octahedral metal centers. Tritopic pyridine ligands incorporating aluminum or gallium, in which the coordination sites for self-assembly are controlled by the metal's octahedral coordination environment, were assembled with appropriately angled (60° or 90°) platinum acceptors and afforded novel heterometallic trigonal-bipyramidal cages. Two trigonal prismatic cages were successfully constructed from the self-assembly of an electron-rich, planar donor, 1,3,5-tris(4-pyridylethynyl)benzene (**9**) with dinuclear ruthenium arene metalloligands, the former possessing two octahedral ruthenium centers capped by *p*-*i*Pr-C_6H_4Me and bridged by either oxalate ($C_2O_4^{2-}$) or 2,5-dihydroxy-1,4-benzoquinonato ($C_6H_2O_4^{2-}$). Furthermore, we have demonstrated that the self-assembly of building blocks possessing ethynyl functionalities can endow the 3-D cages with interesting properties, such as increased electron density and fluorescence. The efficient electron transfer from the self-assembled trigonal prismatic cages to the electron deficient nitroaromatics quenched the fluorescence emission of 3-D cages, demonstrating that the "host" cages may be developed into selective and discriminatory fluorescent sensors for nitroaromatics.

We are confident that the efficient construction of 3-D cages from pre-organized metalloligands via coordination-driven self-assembly will open a door to new supramolecular nanoarchitectures with functional metallic centers. This will allow, for example, the expression of novel magnetic and photophysical properties, as well as catalytic behavior. Furthermore, self-assemblies of functional metalloligands may also find application in the fabrication of stimulus-responsive molecular devices. [8d]

Experimental Section

General Details

Metalloligands **2**,[8e] **10**, and **11**[11a, 11b] were prepared according to reported methods. **1** was synthesized using an analogous procedure to that of **2**. Deuterated solvents were purchased from Cambridge Isotope Laboratory (Andover, MA). NMR spectra were recorded on either a Varian Unity 300 MHz or a Bruker 300 MHz spectrometer. ^{1}H NMR chemical shifts are reported relative to residual solvent signals, and $^{31}P\{^1H\}$ NMR chemical shifts are referenced to an external unlocked sample of 85% H_3PO_4 (δ = 0.0 ppm). Mass spectra for

the self-assemblies were recorded on a Micromass Quattro II triple-quadrupole mass spectrometer using electrospray ionization with a MassLynx operating system. Electronic absorption spectra were recorded on a Perkin Elmer Lambda 750 UV/Visible spectrophotometer. Fluorescence emission studies were carried out on Horiba Jobin Yvon Fluoromax-4 spectrometer. The solvents used for all photophysical studies were of spectroscopic grade and purchased from commercial sources. From a single crystal of **12**, the diffraction data were collected at 100 K on an ADSC Quantum 210 CCD diffractometer with synchrotron radiation (λ = 0.90000 Å) at the Macromolecular Crystallography Beamline 6B1, Pohang Accelerator Laboratory (PAL), Pohang, Korea. The raw data were processed and scaled using the program HKL2000. The structure was solved by direct methods, and the refinements carried out with full-matrix least-squares on F^2 with the appropriate software implemented in the SHELXTL program package.

Synthesis of Tri[1-(4-pyridyl)acetylacetonato]gallium (1)

Sodium bicarbonate (197 mg, 2.35 mmol) was added to a solution of 4-pyridylbutane-1,3-dione (335 mg, 2.05 mmol) and $Ga(NO_3)_2$ (150 mg, 0.58 mmol) in methanol and water (10 mL, v:v = 1:1). After stirring at room temperature for 4 h, a white solid precipitated and was collected by filtration. The crude product was then dissolved in CH_2Cl_2, washed with water, dried over anhydrous sodium sulfate, filtered, and the solvent evaporated under reduced pressure. Then, a ethyl acetate and hexane mixture (20 mL, v:v = 1:1) was added to the residue, precipitating a white solid that was collected by filtration to afford **1** (168 mg). Yield: 52%. ^{1}H NMR (CD_2Cl_2/CD_3NO_2, v:v = 2:1, 300 MHz, 298 K): δ = 8.55 (m, 6H, H_α-Py), 7.63 (m, 6H, H_β-Py), 6.30 (dd, 3H, *J* = 3.3 Hz), 2.15 (m, 9H). Anal. Calcd for $C_{54}H_{48}Ga_2N_6O_{12}$: C, 58.30; H, 4.35; N 7.55; Found: C, 58.56; H, 4.26; N, 7.29.

Synthesis of Trigonal-bipyramidal Cage 5

A CD_2Cl_2 solution (0.60 mL) of Tri[1-(4-pyridyl)acetylacetonato]-gallium (III) (**1**) (2.18 mg, 3.92 μmol) was added dropwise to a CD_3NO_2 solution of **3** (4.29 mg, 5.88 μmol). The mixture was stirred at room temperature for 2 h before being transferred into appropriate vessels for NMR or ESI-MS characterization. The solid product was obtained by removing the solvent *in vacuo*. Yield: 93%. ^{31}P{^{1}H} NMR(CD_2Cl_2/CD_3NO_2, v:v = 2:1, 121.4MHz) δ = −1.4 ppm (s, ^{195}Pt satellites, $^1J_{Pt\text{-}P}$: 3059.2 Hz); ^{1}H NMR (CD_2Cl_2/CD_3NO_2, v:v = 2:1, 300 MHz, 298 K): δ = 8.91 (m, 12H, H_α-Py), 7.95, 7.90 (d, 12H, H_β-Py), 6.23 (s, 6H, enol-H), 2.16 (s, 18H,-CH_3), 1.65–1.75 (m, 36H, PCH_2CH$_3$),1.15–1.25 (m, 54H, PCH$_2$CH_3); MS (ESI) for **5** ($C_{96}H_{138}F_{18}Ga_2N_6O_{30}P_6Pt_3S_6$): m/z: 1500.2 [M – 2OTf]$^{2+}$; 951.2 [M – 3OTf]$^{3+}$; Anal. Calcd for $C_{96}H_{138}F_{18}Ga_2N_6O_{30}P_6Pt_3S_6$: C, 33.93; H, 4.21; N, 2.55; Found: C, 34.13; H, 4.50; N, 2.40.

Synthesis of Trigonal-bipyramidal Cage 6

A CD_2Cl_2 solution (0.60 mL) of Tri[1-(4-pyridyl)acetylacetonato] aluminum (III) (**2**) (2.22 mg, 4.32 μmol) was added dropwise to a CD_3NO_2 solution of **3** (4.73 mg, 6.49 μmol). The mixture was stirred at room temperature for 2 h before being transferred into appropriate vessels for NMR or ESI-MS characterization. The solid product was obtained by removing the solvent under vacuum. Yield: 96%. ^{31}P{^{1}H} NMR (CD_2Cl_2/CD_3NO_2, v:v = 2:1, 121.4MHz) δ = −0.27 ppm (s, ^{195}Pt satellites, $^1J_{Pt\text{-}P}$: 3097.2 Hz); ^{1}H NMR (CD_2Cl_2/CD_3NO_2, v:v = 2:1, 300 MHz, 298 K): δ = 8.90 (m, 12H, H_α-Py), 7.72, 7.92 (d, 12H, H_β-Py), 6.35 (s, 6H, enol-H), 2.15 (s, 18H,-CH_3), 1.70 (m, 36H, PCH_2CH$_3$),1.20 (m, 54H, PCH$_2$CH_3); MS (ESI) for **6** ($C_{96}H_{138}Al_2F_{18}N_6O_{30}P_6Pt_3S_6$): m/z: 1457.8 [M – 2OTf]$^{2+}$; 654.7 [M – 4OTf]$^{4+}$; Anal. Calcd for $C_{96}H_{138}Al_2F_{18}N_6O_{30}P_6Pt_3S_6$: C, 34.86; H, 4.33; N, 2.61; Found: C, 34.63; H, 4.57; N, 2.44.

Synthesis of Trigonal-bipyramidal Cage 7

Tri[1-(4-pyridyl)acetylacetonato]gallium (III) **1** (0.79 mg, 1.42 μmol) and organoplatinum 60° acceptor **4** (2.48 mg, 2.13 μmol) were mixed in an acetone-*d6*/D_2O (v:v = 1:1) solution and kept at 65°C for 12 h before being transferred into appropriate vessels for NMR or ESI-MS characterization. The solid product was obtained by removing the solvent *in vacuo*. Yield: 90%. $^{31}P\{^1H\}$ NMR (acetone-*d6*/D_2O, v:v =1 : 1, 121.4MHz) δ = 14.5 ppm (s, ^{195}Pt satellites, $^1J_{Pt\text{-}P}$: 2670.8 Hz); ^1H NMR (acetone-*d6*/D_2O, v:v = 1:1, 300 MHz, 298 K): δ = 9.32 (m, 12H, H_α-Py), 8.82 (s, 6H), 8.42 (d, 12H, *J* = 6.3 Hz, H_β-Py), 7.97 (m, 6H), 7.85 (m, 12H), 5.70 (s, 6H), 2.55 (s, 18H,-C*H*$_3$), 2.35 (m, 72H, PC*H*$_2$CH$_3$),1.35 (m, 108H, PCH$_2$C*H*$_3$); MS (ESI) for **7** ($C_{168}H_{252}Ga_2N_{12}O_{30}P_{12}Pt_6$): m/z: 1445.8 $[M - 3NO_3]^{3+}$; 1068.8 $[M - 4NO_3]^{4+}$; Anal. Calcd for $C_{168}H_{252}Ga_2N_{12}O_{30}P_{12}Pt_6$: C, 43.85; H, 5.52; N, 3.65; Found: C, 43.96; H, 5.88; N, 3.41.

Synthesis of Trigonal-bipyramidal Cage 8

Tri[1-(4-pyridyl)acetylacetonato] aluminum (III) **2** (1.08 mg, 2.11 μmol) and organoplatinum 60° acceptor **4** (3.67 mg, 3.16 μmol) were mixed in an acetone-*d6*/D_2O (v:v = 1:1) solution and kept at 65°C for 12 h before being transferred into appropriate vessels for NMR or ESI-MS characterization. The solid product was obtained by removing the solvent *in vacuo*. Yield: 92%. $^{31}P\{^1H\}$ NMR (acetone-*d6*/D_2O, v:v = 1:1, 121.4MHz) δ = 11.8 ppm (s, ^{195}Pt satellites, $^1J_{Pt\text{-}P}$: 2658.7 Hz); ^1H NMR (acetone-*d6*/D_2O, v:v = 1:1, 300 MHz, 298 K): δ = 9.05 (m, 12H, H_α-Py), 8.55 (s, 6H), 8.12 (d, 12H, *J* = 6.3 Hz, H_β-Py), 7.70 (m, 6H), 7.56 (m, 12H), 5.40 (s, 6H), 2.26(s, 18H,-C*H*$_3$), 1.52 (m, 72H, PC*H*$_2$CH$_3$), 1.15 (m, 108H, PCH$_2$C*H*$_3$); MS (ESI) for **8** ($C_{174}H_{252}Al_2N_{12}O_{30}P_{12}$): m/z: 1473.4[M – $3NO_3]^{3+}$; 1089.6 $[M - 4NO_3]^{4+}$; Anal. Calcd for $C_{174}H_{252}Al_2N_{12}O_{30}P_{12}$: C, 43.68; H, 5.62; N, 3.72; Found: C, 43.66; H, 5.80; N, 3.52.

Synthesis of Trigonal Prismatic Cage 12

A CD_3NO_2 solution (0.5 mL) of tripodal donor **9** (1.50 mg, 0.004 mmol) was added dropwise to a CD_3OD solution (0.5 mL) of ruthenium triflate acceptor **10** (5.15 mg, 0.006 mmol). The mixture was then stirred for 4 h at room temperature. Upon addition of diethyl ether, a yellow crystalline powder was afforded. Yield 89 %. ^1H NMR (400 MHz, CD_3COCD_3): δ=8.21 (d, $^3J_{H,H}$=6.6 Hz, 12H;Py-H_α), 7.78 (s, 6H ; Hbz), 7.61 (d, $^3J_{H,H}$=6.6 Hz, 12H ; Py-H_β), 6.11 (d, $^3J_{H,H}$ =6.3Hz, 12H; Har), 5.96 (d, $^3J_{H,H}$ = 6.3Hz, 12H; Har), 2.96 (sept, $^3J_{H,H}$ =6.9Hz, 6H; CH), 2.29 (s, 18H; CH3), 1.39 (d, $^3J_{H,H}$ =6.9Hz, 36H; CH_3); MS (ESI) for **12** ($C_{126}H_{114}F_{18}N_6O_{30}Ru_6S_6$): 1517.0 $[M - 2OTf]^{2+}$; 961.7 $[M - 3OTf]^{3+}$; Anal. Calcd for $C_{126}H_{114}F_{18}N_6O_{30}Ru_6S_6$: C, 45.40; H, 3.45; N, 2.52; Found: C, 45.31; H, 3.41; N, 2.50.

Synthesis of Trigonal Prismatic Cage 13

A CD_3NO_2 solution (0.5 mL) of tripodal donor **9** (2.63 mg, 0.007 mmol) was added dropwise to a CD_3OD solution (0.5 mL) of the acceptor **11** (9.37 mg, 0.010 mmol). The mixture was then stirred for 4 h at room temperature. Upon the addition of diethyl ether, a wine red crystalline solid was formed and collected. Yield 83 %. ^1H NMR (400 MHz, CD_3COCD_3): δ=8.45 (d, $^3J_{H,H}$=6.6 Hz, 12H;Py-H_α), 7.84 (s, 6H ; H-bz), 7.65 (d, $^3J_{H,H}$=6.6 Hz, 12H ; Py-H_β), 6.21 (d, $^3J_{H,H}$ =6.3Hz, 12H; H_{Ar}), 6.01 (d, $^3J_{H,H}$ = 6.3Hz, 12H; H_{Ar}), 5.81 (s, 6H; H_q), 3.01 (sept, $^3J_{H,H}$ = 6.92Hz, 6H; CH), 2.26 (s, 18H; CH_3), 1.39 (d, $^3J_{H,H}$ =6.9Hz, 36H; CH_3); MS (ESI) for **13** ($C_{138}H_{120}F_{18}N_6O_{30}Ru_6S_6$): 1592.8 $[M - 2OTf]^{2+}$; 1011.9 $[M - 3OTf]^{3+}$; Anal. Calcd for $C_{138}H_{120}F_{18}N_6O_{30}Ru_6S_6$: C, 47.58; H, 3.47; N, 2.41; Found: C, 47.55; H, 3.44; N, 2.43.

Photophysical Studies of 12 and 13

Fluorescence quenching studies were performed by adding a stock methanol solution of TNT or PA (1.0×10^{-3}) gradually to 2.0 mL methanol solutions of **12** or **13** (1.0×10^{-6} M). The sample was excited at 280 nm and the emission intensity monitored at 350 nm. Analysis of the normalized fluorescence intensity (I_0/I) as a function of increasing quencher concentration ([G]) was well described by the Stern-Volmer equation $I_0/I = 1 + K_{SV}[G]$. The K_{SV} was calculated by fitting the equation to the Stern-Volmer plot.

Supplementary Material

Refer to Web version on PubMed Central for supplementary material.

Acknowledgments

P.J.S. thanks the NIH (Grant GM-057052) for financial support. V.V. and K.W.C. appreciate the financial support of WCU program (R33-2008-000-10003) of National Research Foundation of Korea and the Pohang Accelerator Laboratory (PAL) for X-ray structural analysis.

References

1. (a) Cann, AJ. Principles of Molecular Virlolgy. San Diego: Academic Press; 1993. (b) Uchida M, Klem MT, Allen M, Suci P, Flenniken M, Gillitzer E, Varpness Z, Liepold LO, Young M, Douglas T. Adv. Mater. 2007; 19:1025.
2. (a) Stang PJ, Olenyuk B. Acc. Chem. Res. 1997; 30:502. (b) Leininger S, Olenyuk B, Stang PJ. Chem. Rev. 2000; 100:853. [PubMed: 11749254] (c) Holliday BJ, Mirkin CA. Angew. Chem. Int. Ed. 2001; 40:2022. (d) Seidel SR, Stang PJ. Acc. Chem. Res. 2002; 35:972. [PubMed: 12437322] (e) Fujita M, Tominaga M, Hori A, Therrien B. Acc. Chem. Res. 2005; 38:369. [PubMed: 15835883] (f) Oliver CG, Ulman PA, Wiester MJ, Mirkin CA. Acc. Chem. Res. 2008; 41:1618. [PubMed: 18642933] (h) De S, Mahata K, Schmittel M. Chem. Soc. Rev. 2010; 39:1555. [PubMed: 20419210]
3. (a) Fiedler D, Leung DH, Bergman RG, Raymond KN. Acc. Chem. Res. 2005; 38:349. [PubMed: 15835881] (b) Northrop BH, Yang H-B, Stang PJ. Chem. Commun. 2008:5896. (c) Northrop BH, Chercka D, Stang PJ. Tetrahedron. 2008; 64:11495. [PubMed: 20011029] (d) Parkash MJ, Lah MS. Chem. Commun. 2009:3326. (e) Raymond KN. Nature. 2009; 460:585. (f) Pluth MD, Bergman RG, Raymond KN. Acc. Chem. Res. 2009; 42:1650. [PubMed: 19591461] (g) Lee J, Farha OK, Roberts J, Scheidt KA, Nguyen ST, Hupp JT. Chem. Soc. Rev. 2009; 38:1450. [PubMed: 19384447]
4. (a) Resendiz MJE, Noveron JC, Disteldorf H, Fischer S, Stang PJ. Org. Lett. 2004; 6:651. [PubMed: 14986941] (b) Lin R, Yip JH, Zhang K, Koh LL, Wong KY, Ho KP. J. Am. Chem. Soc. 2004; 126:15852. [PubMed: 15571410] (c) Bar AK, Chakrabarty R, Mostafa G, Mukherjee PS. Angew. Chem. Int. Ed. 2008; 47:8455. (d) Malina J, Hannon MJ, Brabec V. Nucleic Acids Res. 2008; 36:3630. [PubMed: 18467423]
5. (a) Yoshizawa M, Klosterman JK, Fujita M. Angew. Chem. Int. Ed. 2009; 48:3418. (b) He Q-T, Li X-P, Liu Y, Yu Z-Q, Wang W, Su C-Y. Angew. Chem. Int. Ed. 2009; 48:6156. (c) Mal P, Breiner B, Rissanen K, Nitschke JR. Science. 2009; 324:1697. [PubMed: 19556504] (d) Clever, GuidoH; Tashiro, S.; Shionoya, M. Angew. Chem. Int. Ed. 2009; 48:7010. (e) Liao P, Langloss BW, Johnson AM, Knudsen ER, Tham FS, Julian RR, Hooley RJ. Chem. Commun. 2010; 46:4932. (f) Peinador C, Pía E, Blanco VC, García MD, Quintela JM. Org. Lett. 2010; 12:1380. [PubMed: 20218642]
6. (a) Merlau ML, Mejia MDP, Nguyen ST, Hupp JT. Angew. Chem. Int. Ed. 2001; 40:4239. (b) Masar MS, Gianneschi NC, Oliveri CG, Stern CL, Nguyen ST, Mirkin CA. J. Am. Chem. Soc. 2007; 129:10149. [PubMed: 17655295] (c) Lee SJ, Cho SH, Mulfort KL, Tiede DM, Hupp JT, Nguyen ST. J. Am. Chem. Soc. 2008; 130:16828. [PubMed: 19053407] (d) Ulmann PA, Braunschweig AB, Lee OS, Wiester MJ, Schatz GC, Mirkin CA. Chem. Commun. 2009:5121.
7. (a) Yoshizawa M, Tamura M, Fujita M. Science. 2006; 312:251. [PubMed: 16614218] (b) Ghosh K, Yang H-B, Northrop BH, Lyndon MM, Zheng Y-R, Muddiman DC, Stang PJ. J. Am. Chem. Soc. 2008; 130:5320. [PubMed: 18341280] (c) Yang H-B, Ghosh K, Zhao Y, Northrop BH, Lyndon

MM, Muddiman DC, White HS, Stang PJ. J. Am. Chem. Soc. 2008; 130:839. [PubMed: 18166061] (d) Ghosh K, Hu J-M, White HS, Stang PJ. J. Am. Chem. Soc. 2009; 131:6695. [PubMed: 19397325] (e) Zhao L, Ghosh K, Zheng Y-R, Stang PJ. J. Org. Chem. 2009; 74:8516. [PubMed: 19835395] (f) Suzuki K, Takao K, Sato S, Fujita M. J. Am. Chem. Soc. 2010; 132:2544. [PubMed: 20136081] (g) Liu T, Liu Y, Xuan W, Cui Y. Angew. Chem. Int. Ed. 2010; 49:4121. (h) Zheng Y-R, Ghosh K, Yang H-B, Stang PJ. Inorg. Chem. 2010; 49:4747. [PubMed: 20443570]

8. (a) Vreshch VD, Lysenko AB, Chernega AN, Howard JAK, Krautscheid H, Sieler J, Domasevitch KV. Dalton Trans. 2004:2899. [PubMed: 15349164] (b) Müller IM, Möller D. Angew. Chem. Int. Ed. 2005; 44:2969. (c) Tidmarsh IS, Faust TB, Adams H, Harding LP, Russo L, Clegg W, Ward MD. J. Am. Chem. Soc. 2008; 130:15167. [PubMed: 18855358] (d) Duriska MB, Neville SM, Moubaraki B, Cashion JA, Halder GJ, Chapman KW, Balde C, Letard JF, Murray KS, Kepert CJ, Batten SR. Angew. Chem. Int. Ed. 2009; 48:2549. (e) Wu H-B, Wang Q-M. Angew. Chem. Int. Ed. 2009; 48:7343.
9. (a) Benkstein KD, Hupp JT, Stern CL. J. Am. Chem. Soc. 1998; 120:12982. (b) Manimaran B, Thanasekaran P, Rajendran T, Liao R-T, Liu Y-H, Lee G-H, Peng S-M, Rajagopal S, Lu K-L. Inorg. Chem. 2003; 42:4795. [PubMed: 12895097]
10. (a) Han Y-F, Jia W-G, Yu W-B, Jin G-X. Chem. Soc. Rev. 2009; 38:3419. [PubMed: 20449060] (b) Therrien B. Eur. J. Inorg. Chem. 2009:2445.
11. (a) Yan H, Suss-Fink G, Neels A, Stoeckli-Evans H. Dalton Trans. 1997:4345. (b) Therrien B, Suss-Fink G, Govindaswamy P, Renfrew AK, Dyson PJ. Angew. Chem. Int. Ed. 2008; 47:3773. (c) Govindaswamy P, Suss-Fink G, Therrien B. Organometallics. 2007; 26:915. (d) Mattson J, Govindaswamy P, Renfrew AK, Dyson PJ, Stepnicka P, Suss-Fink G, Therrien B. Organometallics. 2009; 28:4350. (e) Mattsson J, Govindaswamy P, Furrer J, Sei Y, Yamaguchi K, Suess-Fink G, Therrien B. Organometallics. 2008; 27:4346.
12. (a) Zhao L, Ghosh K, Zheng Y-R, Lyndon MM, Williams TI, Stang PJ. Inorg. Chem. 2009; 48:5590. [PubMed: 19476323] (b) Zhao L, Northrop BH, Stang PJ. J. Am. Chem. Soc. 2008; 130:11886. [PubMed: 18702485]
13. (a) Ikeda A, Yoshimura M, Udzu H, Fukuhara C, Shinkai S. J. Am. Chem. Soc. 1999; 121:4296. (b) Claessens CG, Torres T. Chem. Commun. 2004:1298.
14. (a) Radhakrishnan U, Schweiger M, Stang PJ. Org. Lett. 2001; 3:3141. [PubMed: 11574015] (b) Yang H-B, Ghosh K, Das N, Stang PJ. Org. Lett. 2006; 8:3991. [PubMed: 16928056] (c) Yang H-B, Ghosh K, Arif AM, Stang PJ. J. Org. Chem. 2006; 71:9464. [PubMed: 17137374] (d) Yang H-B, Ghosh K, Northrop BH, Stang PJ. Org. Lett. 2007; 9:1561. [PubMed: 17378574] (e) Yang H-B, Ghosh K, Northrop BH, Stang PJ. Org. Lett. 2007; 9:1561. [PubMed: 17378574]
15. (a) Tarkanyi G, Jude H, Palinkas G, Stang PJ. Org. Lett. 2005; 7:4971. [PubMed: 16235935] (b) Caskey DC, Yamamoto T, Addicott C, Shoemaker RK, Vacek J, Hawkridge AM, Muddiman DC, Kottas GS, Michl J, Stang PJ. J. Am. Chem. Soc. 2008; 130:7620. [PubMed: 18491898] (c) Vacek J, Caskey DC, Horinek D, Shoemaker RK, Stang PJ, Michl J. J. Am. Chem. Soc. 2008; 130:7629. [PubMed: 18491897] (e) Zhao L, Ghosh K, Zheng Y-R, Stang PJ. J. Org. Chem. 2009; 74:8516. [PubMed: 19835395]
16. Han Y-F, Lin Y-J, Jia W-G, Wang G-L, Jin G-X. Chem. Commun. 2008:1807.
17. (a) Ghosh S, Gole B, Bar AK, Mukherjee PS. Organometallics. 2009; 28:4288. (b) Ghosh S, Mukherjee PS. Organometallics. 2008; 27:316.
18. (a) Toal SJ, Trogler WC. J. Mater. Chem. 2006; 16:2871. (b) Swager TM. Acc. Chem. Res. 2008; 41:1181. [PubMed: 18759462] (c) Germain ME, Knapp MJ. Chem. Soc. Rev. 2009; 38:2543. [PubMed: 19690735]

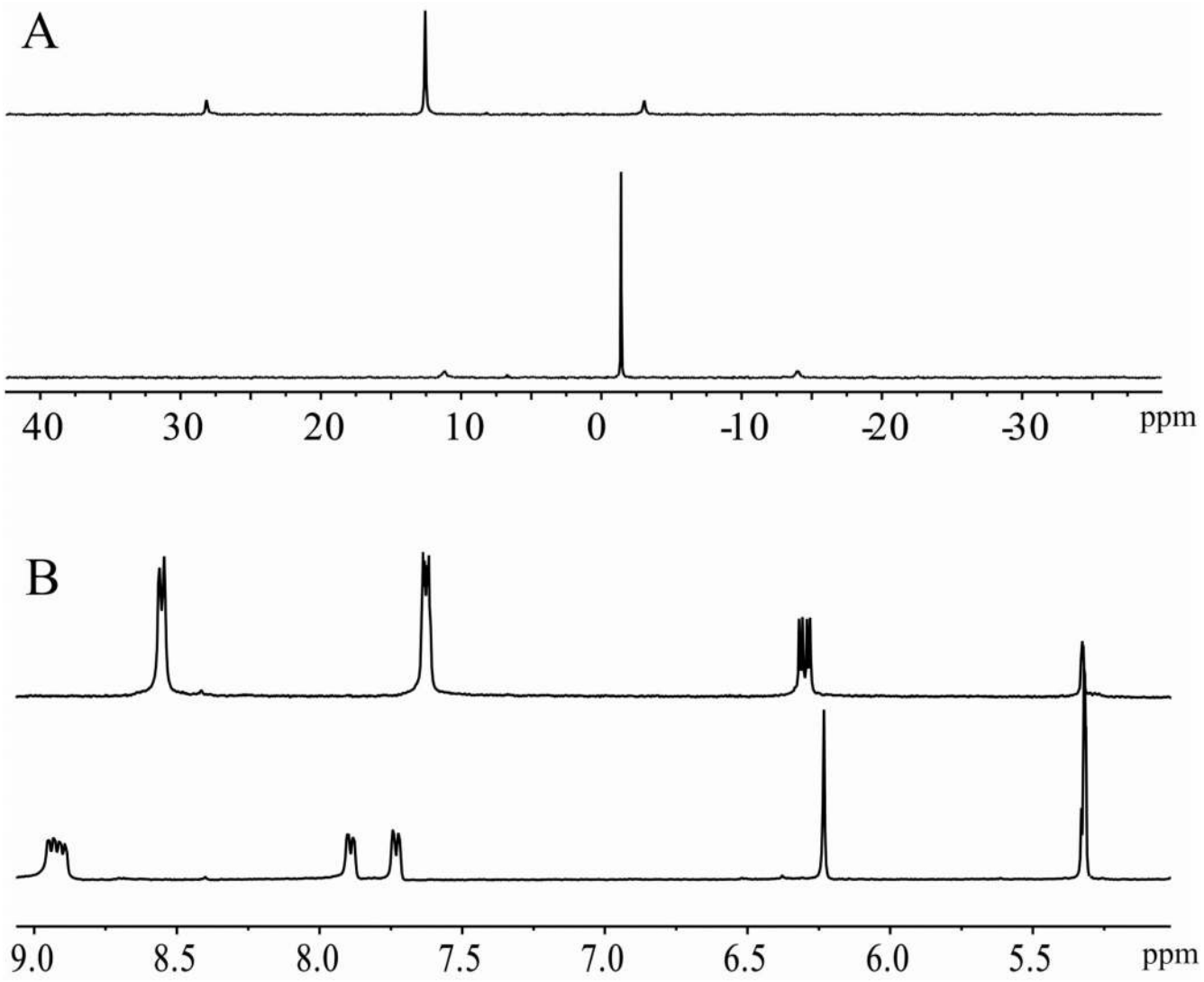

Figure 1.
A) The $^{31}P\{^{1}H\}$ NMR spectra of starting 90° platinum acceptor **3** (*top*) and the trigonal-bipyramidal cage **5** (*bottom*); B) Partial ^{1}H NMR (300 MHz, 298 K) of donor **1** (*top*) and trigonal-bipyramidal cage **5** (*bottom*). All NMR spectra were recorded in CD_2Cl_2/CD_3NO_2 (v:v = 2:1).

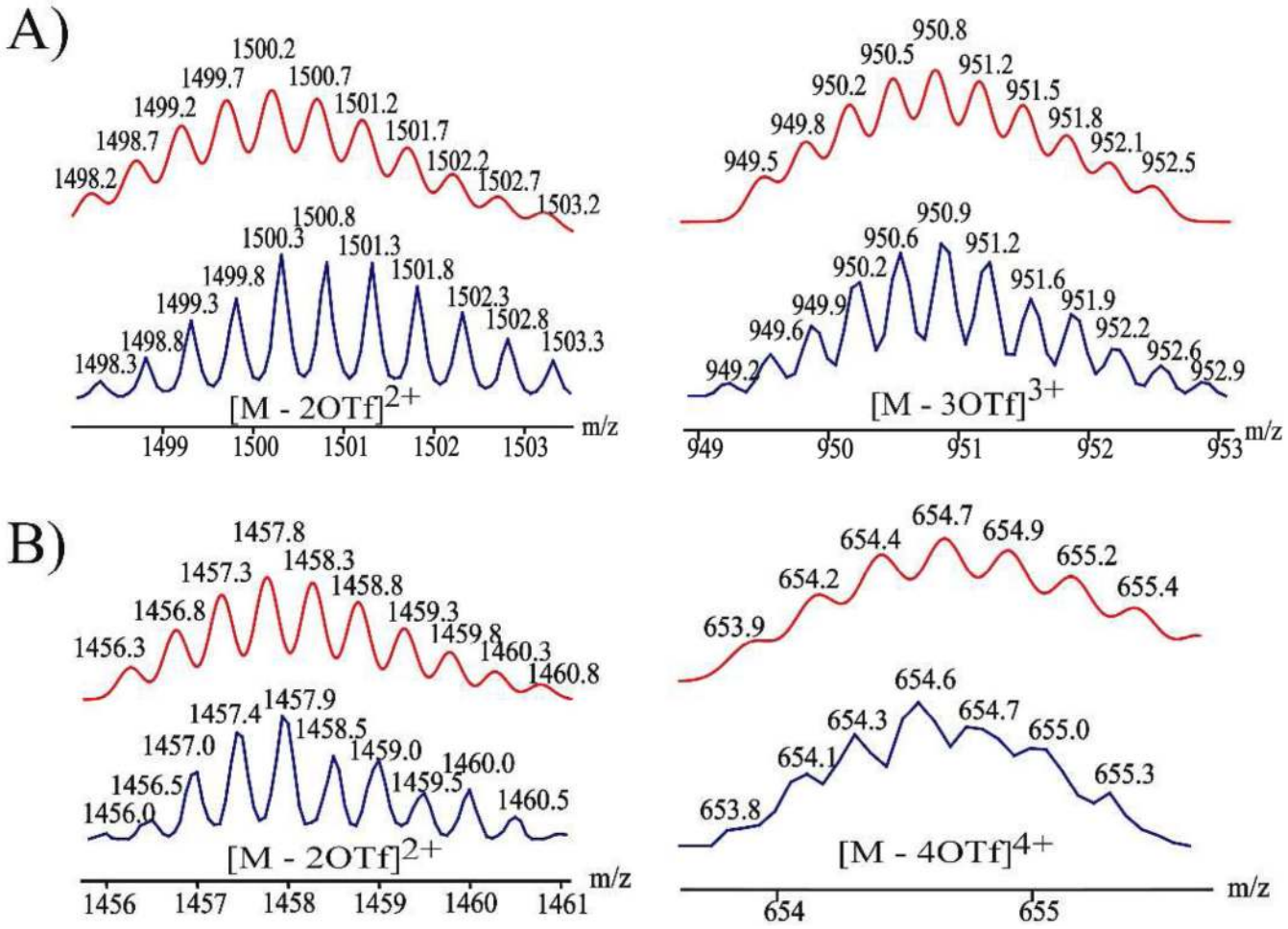

Figure 2.
Calculated (*red*) and experimental (*blue*) ESI mass spectra of trigonal-bipyramidal cages **5** (A) and **6** (B).

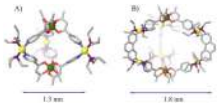

Figure 3.
Proposed structure of the heterometallic, trigonal-bipyramidal cages **5** (A) and **7** (B) as obtained by MM2 force-field simulation.

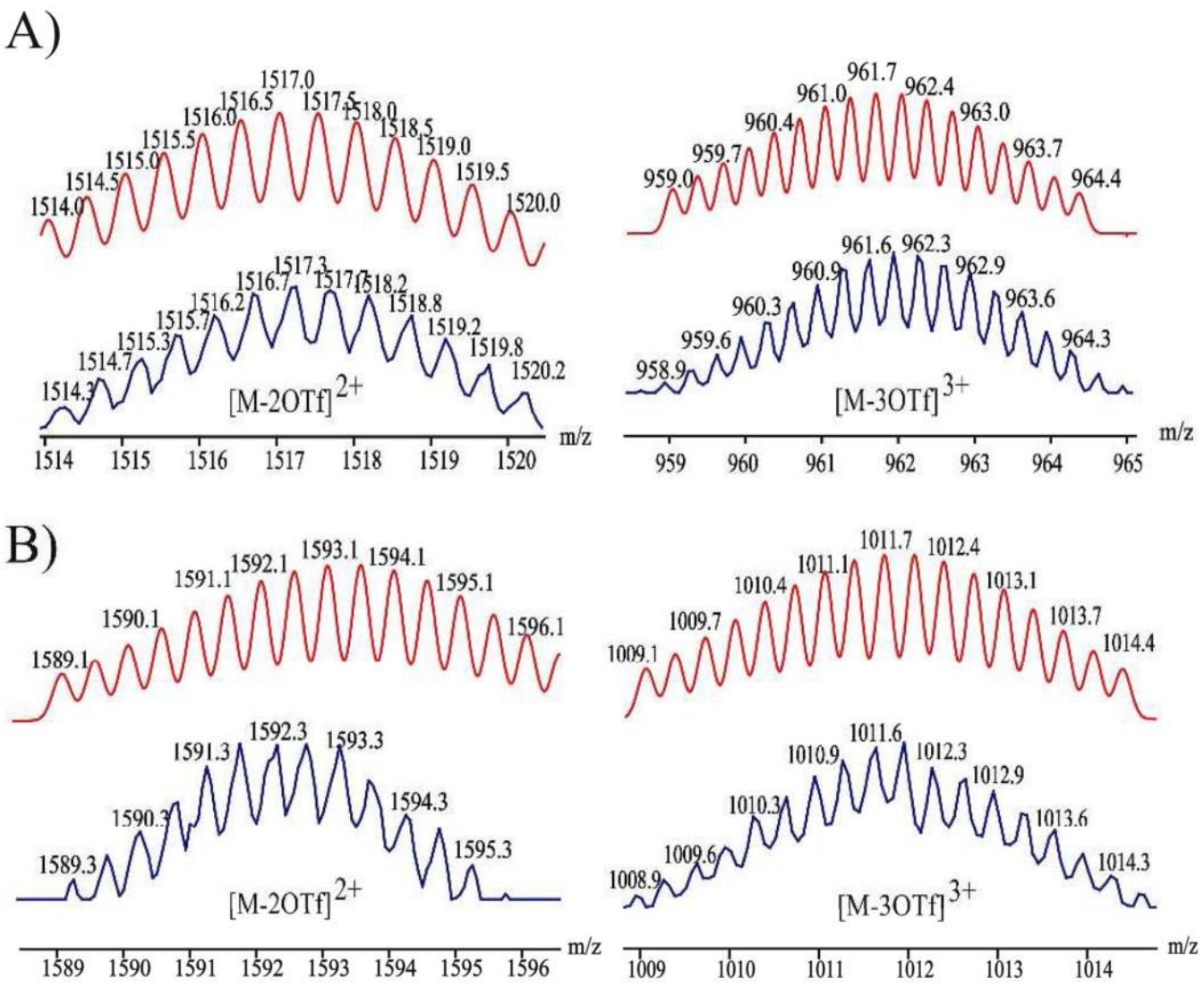

Figure 4.
Calculated (*red*) and experimental (*blue*) ESI mass spectra of trigonal prismatic cages **12** (A) and **13** (B).

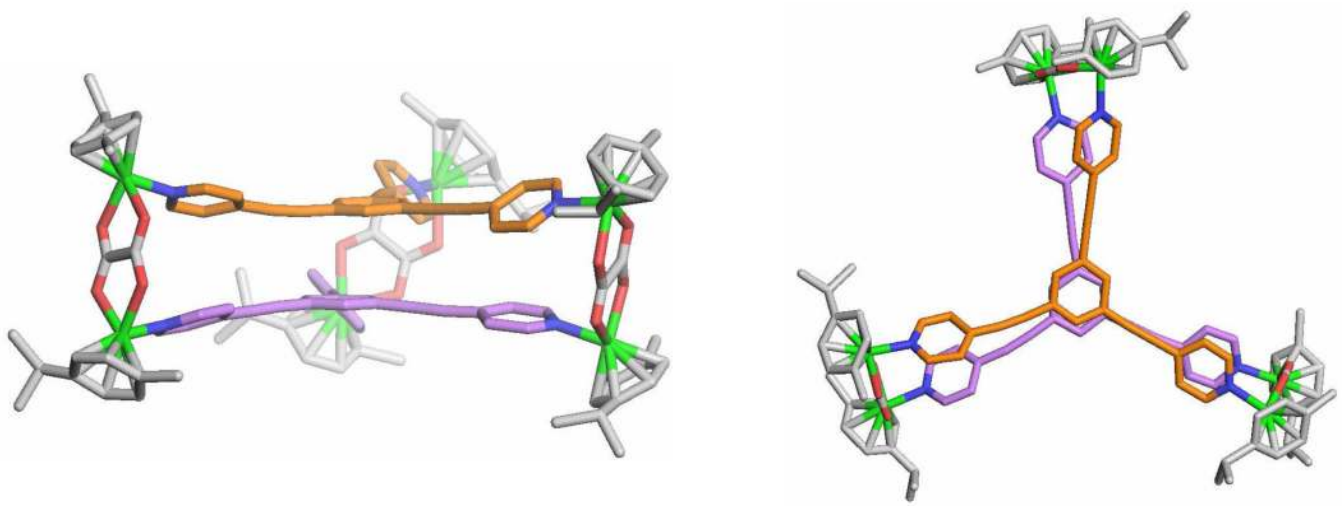

Figure 5.
X-ray structures of the trigonal prismatic cage **12**. Side view (*left*) and top view (*right*). (green = Ru, red = O, blue = N; H-atoms, counter anions and solvent molecules are omitted for clarity).

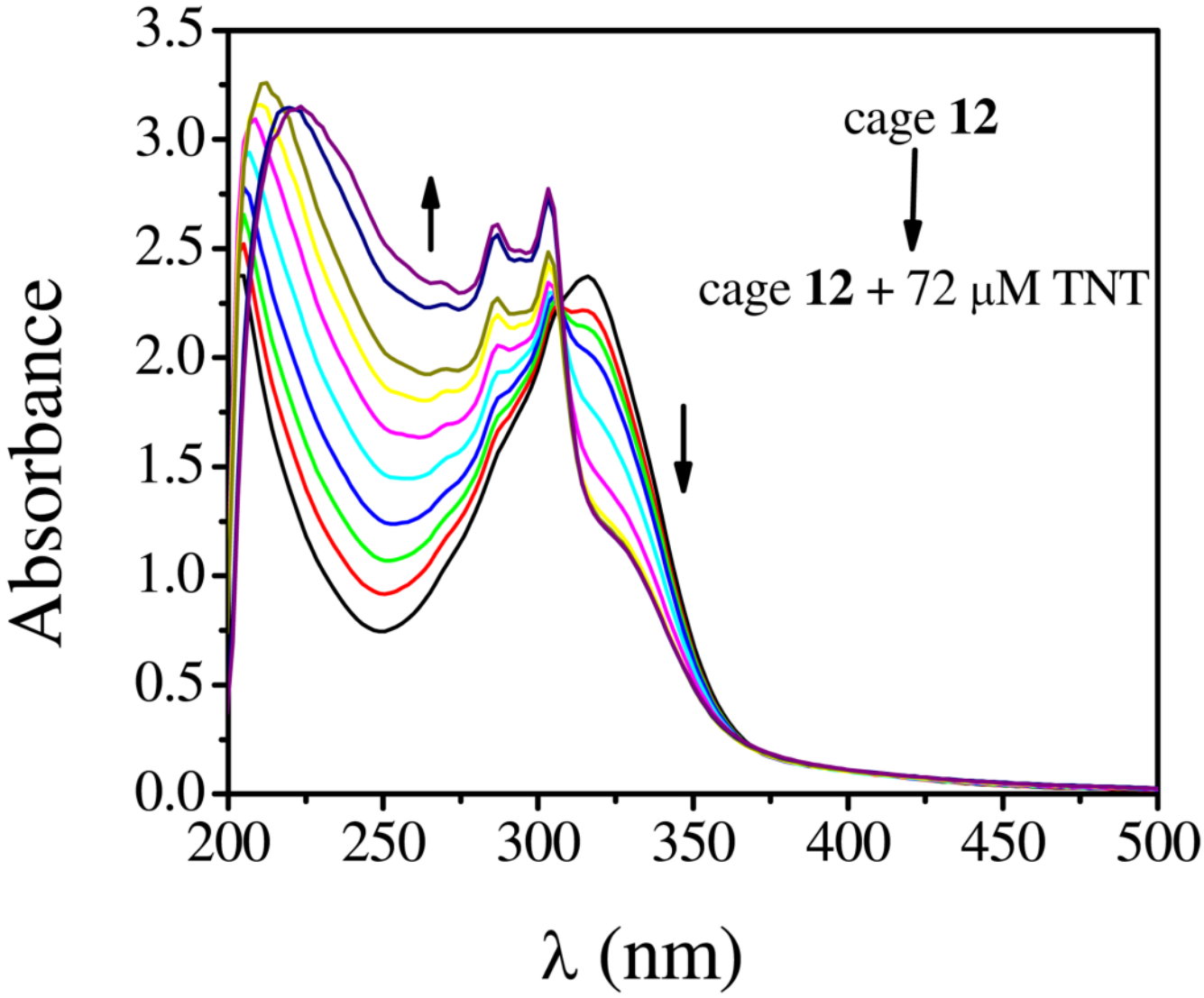

Figure 6.
UV-Vis spectra of **12** (1.0×10^{-5} M solution in methanol) in the presence of TNT (from 0 to 72 μM).

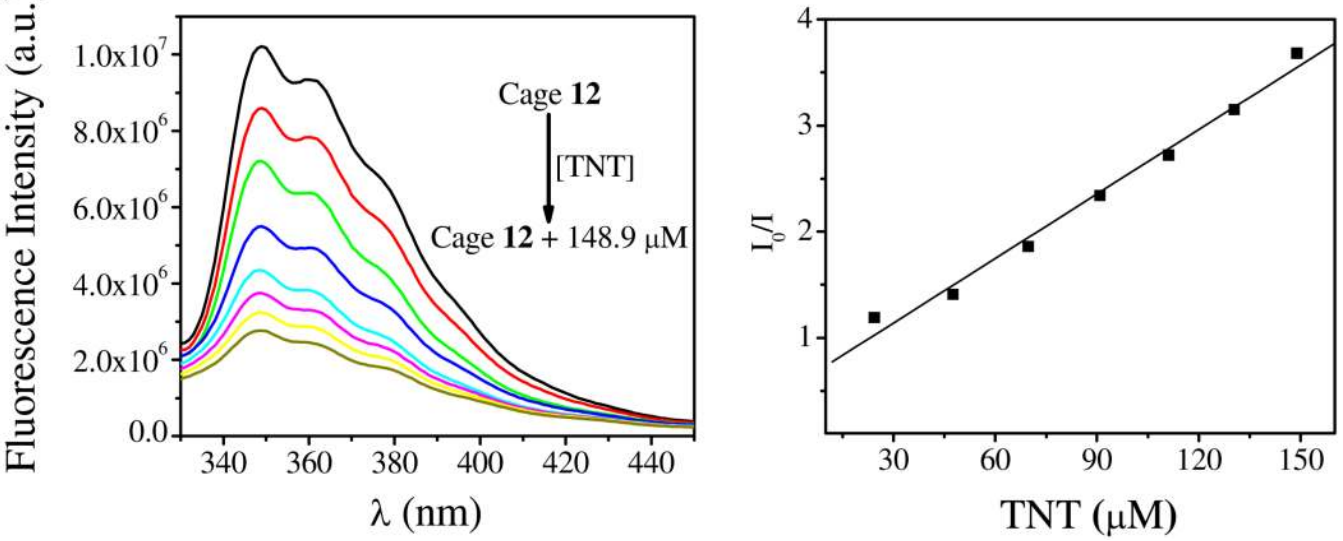

Figure 7.

Fluorescence spectra of **12** (1.0×10^{-6} M in methanol) in the presence of TNT (from 0 to 175 μM), λ_{ex} = 280 nm (*left*); Stern-Volmer plot of fluorescence quenching of **12** by TNT. The fluorescence intensity was monitored at 350 nm (*right*).

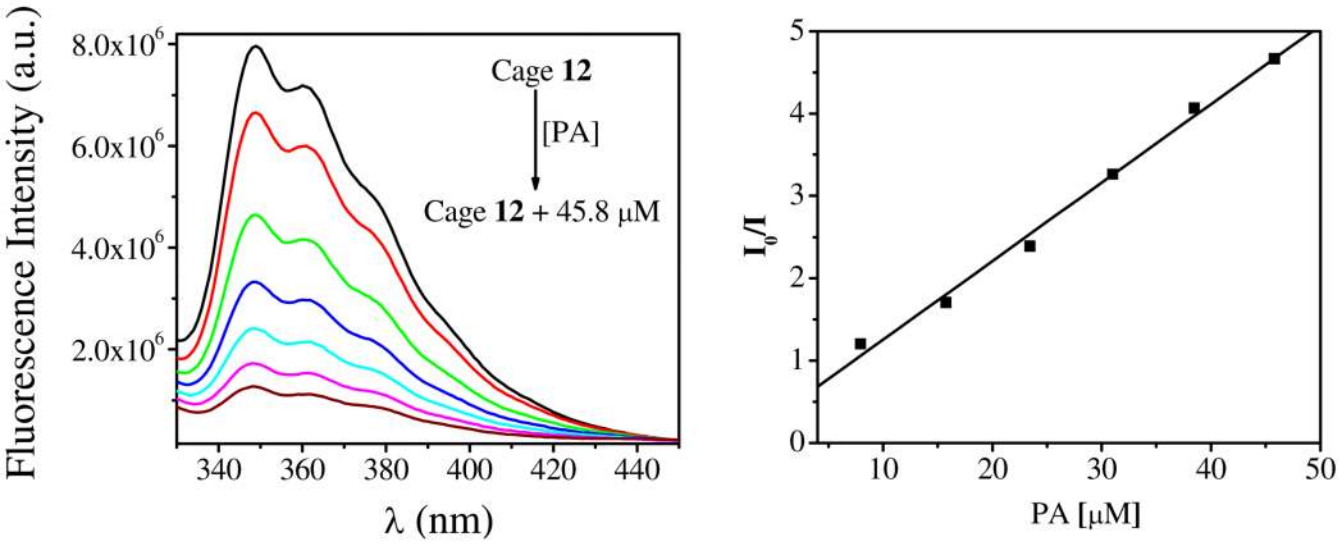

Figure 8.

Fluorescence quenching of **12** by picric acid (*left*) and corresponding Stern-Volmer plot (*right*). Fluorescence spectra were recorded using solutions of **12** (1×10^{-6} M) in methanol monitored at 350 nm.

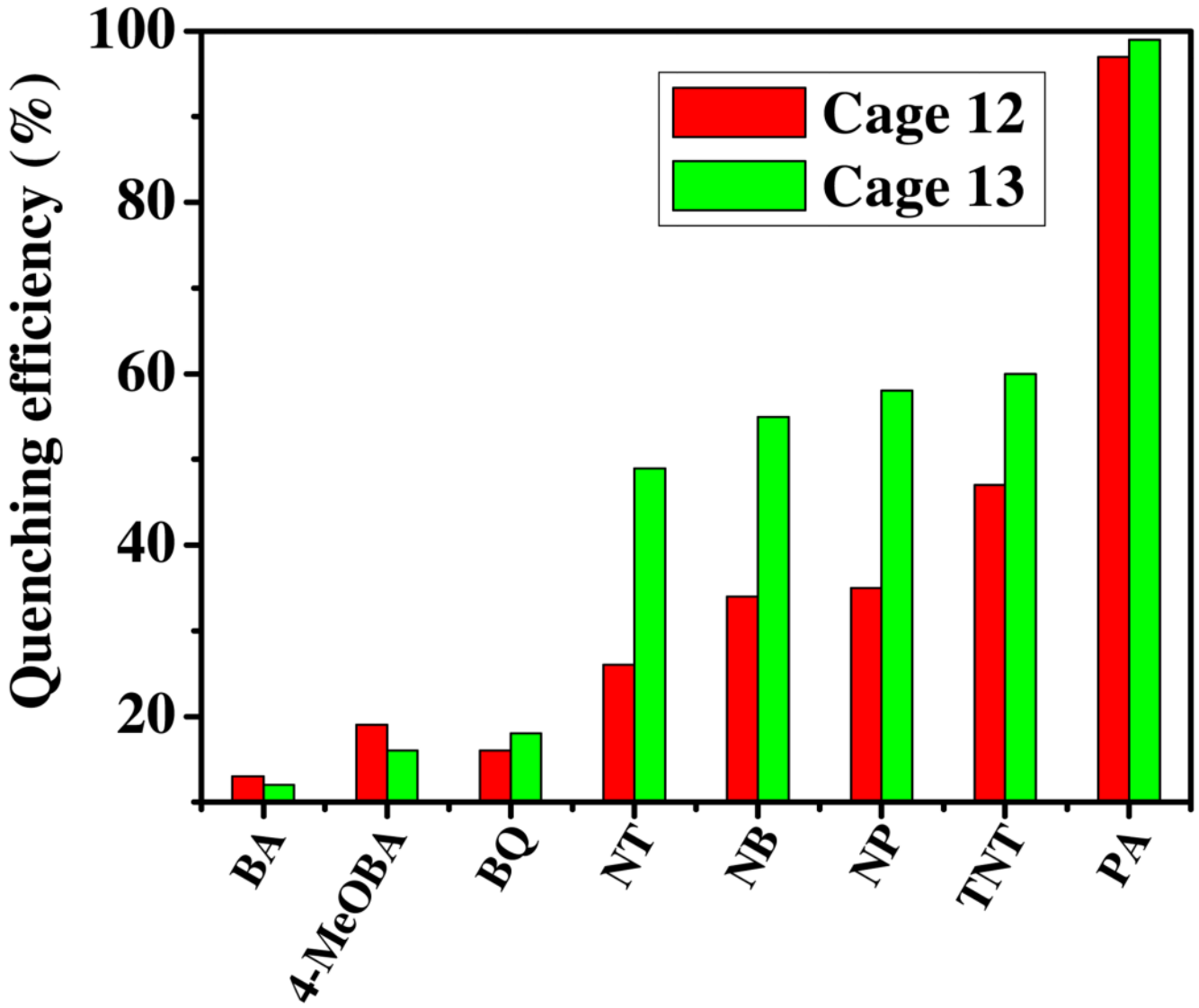

Figure 9.
Selective fluorescent detection of nitroaromatics using coordinated trigonal prismatic cages **12** and **13**. Fluorescence intensity of solutions of **12** and **13** (1.0×10^{-6} M in methanol) were monitored at 350 nm.

Scheme 1.
Coordination-driven self-assembly of M_3L_2 cages from metalloligands with octahedral metal centers.